

See discussions, stats, and author profiles for this publication at: <https://www.researchgate.net/publication/7308349>

# Amphotericin B Encapsulated in Micelles Based on Poly(ethylene oxide)- b lock -poly( l -amino acid) Derivatives Exerts Reduced in Vitro Hemolysis but Maintains Potent in Vivo Antif...

ARTICLE *in* BIOMACROMOLECULES · MAY 2003

Impact Factor: 5.75 · DOI: 10.1021/bm0257614 · Source: PubMed

---

CITATIONS

63

---

READS

32

3 AUTHORS, INCLUDING:



Glen S Kwon

University of Wisconsin-Madison

137 PUBLICATIONS 8,091 CITATIONS

SEE PROFILE

# Amphotericin B Encapsulated in Micelles Based on Poly(ethylene oxide)-*block*-poly(L-amino acid) Derivatives Exerts Reduced in Vitro Hemolysis but Maintains Potent in Vivo Antifungal Activity

Monica L. Adams,<sup>†</sup> David R. Andes,<sup>‡</sup> and Glen S. Kwon<sup>\*†</sup>

Division of Pharmaceutical Sciences, School of Pharmacy, University of Wisconsin—Madison, 777 Highland Avenue, Madison, Wisconsin 53705-2222, and Section of Infectious Diseases, Department of Medicine, University of Wisconsin—Madison School of Medicine, H4/572 Clinical Science Center, 600 Highland Avenue, Madison, Wisconsin 53792-2454

Received December 11, 2002; Revised Manuscript Received February 6, 2003

The core-forming blocks of amphiphilic diblock copolymers based on methoxypoly(ethylene oxide)-*block*-poly(L-aspartate), PEO-*b*-p(L-Asp), were derivatized to incorporate stearate side chains. The effects of stearate esterification were assessed in terms of micelle stability and amphotericin B (AmB) encapsulation/release. The level of stearate esterification modulates the relative self-aggregation state of encapsulated AmB as evidenced by absorption spectroscopy. When AmB is physically loaded into polymeric micelles, the onset of hemolytic activity toward bovine erythrocytes is delayed relative to that of the free drug. Furthermore, the extent of esterification (0, 46, or 91%) appears to have profound influence on the time-dependent hemolytic profile of AmB toward bovine erythrocytes. Particularly in the case of highly substituted stearate ester micelles, incomplete and gradual build-up of hemolysis was observed over a period of 24 h. On the basis of the corresponding absorption spectra, we speculate that encapsulated AmB may interact strongly with stearate side chains, resulting in sustained release. In a neutropenic murine model of disseminated candidiasis, kidney colony-forming unit determination revealed dose-dependent efficacy for the polymeric micelle/AmB formulation, which was not significantly different from that of Fungizone at doses of 0.2, 0.3, and 0.6 mg/kg ( $p = 0.7$ ). Thus, AmB administered via a polymeric micelle formulation retained potent in vivo activity.

## Introduction

Systemic mycoses are increasing in frequency among immunocompromised AIDS, surgery, transplant, and cancer patients. Amphotericin B (AmB), an amphiphilic polyene macrolide, is the therapy of choice for treating systemic fungal infection.<sup>1–4</sup> Parenteral administration of Fungizone, in which AmB is solubilized by sodium deoxycholate, is the most common treatment for systemic mycoses. Although an effective fungicide, Fungizone is often associated with significant toxicities.<sup>2</sup> Due to high toxicities and poor prognosis, there is great need for new, safe, and effective AmB formulations for treatment of systemic mycoses.

There has been immense interest in the development of alternative, lipid-based AmB formulations. AmB lipid complex (Abelcet) and conventional liposomal AmB (AmBisome) are characterized by a substantial reduction in toxicity and an increase in the therapeutic window of AmB.<sup>2,5,6</sup> However, these formulations are also characterized by a considerable loss in antifungal activity. Another

promising approach to the treatment of deep mycoses is administration of AmB encapsulated by long-circulating liposomes.<sup>7</sup> Due to prolonged in vivo residence times, long-circulating liposomes containing AmB are more effective than conventional liposomal AmB against systemic mycoses in murine models.<sup>7–10</sup> These delivery systems incorporate lipids which have been PEGylated, i.e., tethered with poly(ethylene glycol) chains, to impart “stealth” properties and long residence time in biological milieu. AmB loaded into stealth liposome carriers, prepared using PEGylated distearoylphosphatidylethanolamine, is effective in vivo against *Candida albicans*.<sup>11</sup>

Polymeric micelles are often employed for drug delivery purposes and are prepared from amphiphilic block copolymers, which organize in aqueous medium to yield nanoscopic structures with characteristic core/shell architecture.<sup>12,13</sup> The interface formed by the hydrophilic blocks protects the hydrophobic domain against further aggregation and protein recognition/adherence. Similarly, entrapment in polymeric micelles may protect drug molecules from hydrolysis, aggregation, and precipitation by minimizing contact between encapsulated compounds and the bulk aqueous phase. A polymeric micelle formulation may have several distinct advantages over lipid-based AmB formulations, including increased thermodynamic and kinetic stability, high surface

\* To whom correspondence may be addressed. Phone: (608) 265-5183. Fax: (608) 262-3397. E-mail: gsk@pharmacy.wisc.edu.

<sup>†</sup> Division of Pharmaceutical Sciences, School of Pharmacy, University of Wisconsin—Madison.

<sup>‡</sup> Section of Infectious Diseases, Department of Medicine, University of Wisconsin—Madison School of Medicine.

density of long poly(ethylene oxide) (PEO) chains, nanoscopic dimensions, and relative ease of preparation. High thermodynamic and kinetic stability may lead to superior stability toward in vivo dilution. High PEO surface density and long PEO chain length are known to impart steric stability and minimize protein adsorption to hydrophobic surfaces.<sup>14</sup> Moreover, long PEO chains decrease uptake by the reticuloendothelial system and prolong circulation time of polymeric micelles.<sup>15</sup> Due to the nanoscopic dimensions of polymeric micelles, micellar formulations may be easily sterilized by filtration. A polymeric micelle formulation might provide a long-circulating nanodepot of AmB, which may be capable of releasing drug slowly over time.

Recently, a polymeric micelle system based on poly(ethylene oxide)-*block*-poly(*N*-hexyl-L-aspartamide) acyl esters has been developed.<sup>16,17</sup> In this system, the core region consists of a poly(L-aspartate) block which has been derivatized to incorporate acyl chains. The attached acyl chains approximate lipid moieties in terms of their chemical structure. Previous efforts demonstrated that poly(ethylene oxide)-*block*-poly(*N*-hexyl-L-aspartamide)-stearic acid, PEO-*b*-p(HASA), ester micelles encapsulate AmB in a relatively non-self-aggregated state and delay the onset of hemolysis compared to free AmB.<sup>18,19</sup> Delayed hemolytic activity might result from slow, or sustained, release of AmB from PEO-*b*-p(HASA) micelles. As fungal cells are more susceptible to low concentrations of AmB than mammalian cells, gradual release of AmB could potentially impart increased selectivity. The present work examines the effects of experimental loading conditions on AmB encapsulation by PEO-*b*-p(HASA) micelles. The effects of esterification at 0, 46, and 91% stearate attachment on the relative self-aggregation state of AmB and micelle stability are explored. In addition, the concept of sustained release is addressed via time-dependent hemolysis of bovine erythrocytes. Finally, efficacy in a neutropenic murine model of disseminated candidiasis is investigated.

## Experimental Section

**Materials.** Dichloromethane (CH<sub>2</sub>Cl<sub>2</sub>) and D-(+)-trehalose dihydrate were purchased from Sigma (St. Louis, MO). Deuterated chloroform (CDCl<sub>3</sub>), deuterated dimethyl sulfoxide (DMSO-*d*<sub>6</sub>), *N,N*-dimethylformamide (DMF), (dimethylamino)pyridine (DMAP), 6-amino-1-hexanol (6-AH), 2-hydroxypyridine (2-HP), stearic acid, and molecular sieves (4 Å) were purchased from Aldrich (Milwaukee, WI). CH<sub>2</sub>Cl<sub>2</sub> was dried with molecular sieves, and DMF was distilled under vacuum prior to use. Methanol (MeOH) was purchased from Fisher Scientific (Fair Lawn, NJ). Dicyclohexylcarbodiimide (DCC) was purchased from Lancaster (Windham, NH). Amphotericin B (AmB) was obtained from Chem-Impex (Wood Dale, IL). Dimethyl sulfoxide (DMSO) was purchased from Fisher Scientific (Pittsburgh, PA). Methoxypoly(ethylene oxide)-*block*-poly( $\beta$ -benzyl-L-aspartate) was provided by NanoCarrier (Kashiwa, Japan). A clinical bloodstream isolate of *Candida albicans* (K-1) was used for in vivo efficacy experiments. Sabouraud dextrose agar (SDA) slants were from Difco Laboratories (Detroit, MI). Fungizone

was obtained from Bristol-Myers Squibb (Princeton, NJ) and stored at -70 °C until use. All chemicals were reagent grade or above and used without additional purification unless stated otherwise.

**Polymer Preparation.** The preparations of poly(ethylene oxide)-*block*-poly(6-hydroxylhexyl-L-aspartamide), PEO-*b*-p(6-HHA), and poly(ethylene oxide)-*block*-poly(*N*-hexyl-L-aspartamide)-stearic acid ester, PEO-*b*-p(HASA), were described previously.<sup>17</sup> Briefly, methoxypoly(ethylene oxide)-*block*-poly( $\beta$ -benzyl-L-aspartate), PEO-*b*-PBLA, containing a 12 000 g/mol PEO block and an average of 25 L-Asp repeat units was reacted for 24 h at ambient temperature with excess 6-AH in DMF in the presence of 2-HP. PEO-*b*-p(6-HHA) was precipitated in cold isopropyl alcohol and collected by centrifugation. The pellet was washed with cold isopropyl alcohol, followed by chilled ether. The product was dissolved in distilled water and freeze-dried (Labconco, St. Louis, MO). Approximately 5 mg of sample was dissolved in 650  $\mu$ L of DMSO-*d*<sub>6</sub> and loaded into a 5 mm 535-pp Wilmad NMR tube (Buena, NJ). Spectra were acquired on a Varian 500 MHz spectrometer (Palo Alto, CA) equipped with a 5 mm broad-band probe tuned for proton acquisition and referenced to the solvent multiplet at 2.5 ppm. The loss of the aromatic protons attributed to the phenyl group was observed (spectra not shown). To determine the percent substitution, the methylene resonances centered at 1.25 and 1.40 ppm were integrated relative to the PEO polyether methylene peak at 3.6 ppm. The percent yield for the aminolysis product was 94%.

PEO-*b*-p(6-HHA) was reacted with either 0.5 or 5 equiv of stearic acid in CH<sub>2</sub>Cl<sub>2</sub> in the presence of excess DCC and DMAP at ambient temperature for 5 days. The products were collected as described above. Approximately 5 mg of each conjugate was dissolved in 650  $\mu$ L of CDCl<sub>3</sub>. <sup>1</sup>H NMR spectra were acquired as described above and referenced to the solvent singlet at 7.24 ppm. Comparisons between the relative intensity of the PEO peak and the terminal methyl peak of the stearate chains at 0.9 ppm (spectra not shown) allowed determination of the substitution levels. The final products were prepared in 90% yield.

**Encapsulation of AmB.** To determine the effects of stearate esterification on drug loading, 80 mg of PEO-*b*-p(6-HHA) or 5 mg of PEO-*b*-p(HASA), 46 or 91% was dissolved in 2.0 mL of methanol containing 625  $\mu$ g of AmB. Distilled water (d.H<sub>2</sub>O) was added dropwise to the stirring solutions at a rate of 0.075–0.090 mL/min (1 drop/10–12 s) to obtain a 50:50 MeOH/H<sub>2</sub>O mixture. An additional 1.0 mL of d.H<sub>2</sub>O was added to the stirring solutions, followed by 0.75 g of trehalose dihydrate. In the case of PEO-*b*-p(6-HHA), only 0.6 g of trehalose dihydrate was added. The lyoprotectant was dissolved before MeOH was removed, and the volume was reduced to approximately 1.5 mL via rotary evaporation. The aqueous solutions were collected and diluted to a final volume of 5.0 mL with d.H<sub>2</sub>O for all polymers except PEO-*b*-p(6-HHA), which was diluted to 4.0 mL. An additional 0.25 g of trehalose dihydrate was added to the aqueous PEO-*b*-p(HASA) solutions and dissolved by stirring. In the case of PEO-*b*-p(6-HHA), only 0.2 g of trehalose dihydrate was added. The aqueous polymer solutions

contained 18% trehalose and were sterile filtered (0.22  $\mu\text{m}$ , ISC BioExpress; Kaysville, UT). Aliquots (0.5 mL) were immersed in  $\text{N}_2(\text{l})$  until frozen and freeze-dried. To assess the effects of loading conditions on the encapsulation and relative aggregation state of AmB, AmB-loaded PEO-*b*-p(HASA), 91% micelles were prepared as described above in the presence of 625 or 1250  $\mu\text{g}$  of AmB at different solvent volumes (Table 2). Freeze-dried samples containing AmB were shielded from light. "Blank" micelles, in which AmB was omitted, were prepared as described above. All samples were stored over desiccant at 5  $^{\circ}\text{C}$  until use.

**Determination of Micelle Size and Stability by Gel Permeation Chromatography (GPC).** Measurements were performed on an Agilent 1100 series high-performance liquid chromatography system equipped with a refractive index detector. Freeze-dried PEO-*b*-p(6-HHA) and PEO-*b*-p(HASA) micelles, with and without AmB, were reconstituted to 10.0 and 0.5 mg/mL polymer, respectively, with 1.0 mL of phosphate-buffered 155 mM saline, pH = 7.2 (PBS). Reconstituted polymeric micelles were injected (100  $\mu\text{L}$ ) in duplicate on a Shodex SB-806M HQ OHPak size exclusion column equipped with a Shodex OHPak SB-G guard column (Showa Denko, New York, NY). The column was equilibrated with PBS mobile phase and calibrated with dextran molecular weight standards of  $1\text{--}7 \times 10^6$  g/mol (JM Science, Grand Island, NY). The flow rate and column compartment temperature were set to 0.8 mL/min and 37  $^{\circ}\text{C}$ , respectively. The weight-averaged molecular weight ( $M_w$ ), number-averaged molecular weight ( $M_n$ ), and polydispersity ( $D$ ) were calculated with Agilent GPC analysis software (G2071-AA).

**Determination of Drug Content and Relative Aggregation State in AmB-Loaded Polymeric Micelles by Absorption Spectroscopy.** The freeze-dried formulations were reconstituted with 1.0 mL of d.H<sub>2</sub>O. To quantify AmB content, the reconstituted aqueous polymeric micelle solutions were diluted 2-fold with DMF and then diluted appropriately with 50:50 DMF/d.H<sub>2</sub>O. AmB was quantified via absorbance of monomeric AmB at 412–413 nm. The relative aggregation state of AmB was also determined by absorption spectroscopy. In this case, the polymeric micelle formulations were reconstituted in d.H<sub>2</sub>O and diluted 4-fold for all samples except that containing the highest level of AmB, which was diluted 8-fold. All spectra were collected from 320.0 to 450.0 nm with a 1.0 cm path length at a rate of 405 nm/min and a scan step of 0.1 nm.

**Hemolysis of Bovine Erythrocytes.** EDTA-anticoagulated bovine blood was diluted in PBS. Erythrocytes were collected by centrifugation for 10 min at 3000 rpm. The supernatant was removed, and the packed cell volume (PCV) was washed three more times with PBS. The PCV was diluted appropriately in PBS to obtain suspensions containing  $8 \times 10^7$  and  $1.48 \times 10^8$  cells/mL. Cell counts were performed using an Improved Neubauer Brightline hemacytometer (depth = 0.1 mm) from Hausser Scientific (Horsham, PA). The polymeric micelle formulations and blanks were brought to room temperature and reconstituted with 1.0 mL of PBS just prior to use. A 1.85 mL volume of the  $8 \times 10^7$  cells/mL suspension was incubated at 37  $^{\circ}\text{C}$  in a shaking water bath (75 rpm) with 0.15 mL of AmB/polymeric micelle formula-

tion, polymeric micelle blank, or buffer for 24 h. The final cell concentration was  $7.2 \times 10^7$  erythrocytes/mL. Samples, blanks, and controls were withdrawn in triplicate at 1, 9, 16, and 24 h and centrifuged at 3000 rpm for 10 min. Supernatant hemoglobin content was determined via absorbance at 542 nm. The value for total lysis was obtained by hypotonic hemolysis. Percent hemolysis is reported by  $100 - (\text{Abs}_S - \text{Abs}_B)/(\text{Abs}_L - \text{Abs}_B)$  where  $\text{Abs}_S$  is the absorbance of the sample,  $\text{Abs}_B$  is the average absorbance of the buffer, and  $\text{Abs}_L$  is the average absorbance of the lysed samples. All values are reported as mean  $\pm$  standard deviation.

An 8 mg/mL AmB in DMSO stock solution was prepared. To determine the time-dependent hemolytic activity of free drug as a function of concentration, 11.4, 20.4, and 34.0  $\mu\text{L}$  aliquots of the stock solution were diluted to 25.0 mL with PBS to prepare 3.7, 6.5, and 10.9  $\mu\text{g}/\text{mL}$  AmB in PBS solutions containing 0.23, 0.41, and 0.68% DMSO, respectively. One milliliter of each AmB in PBS solution was then incubated with 1.0 mL of the  $1.48 \times 10^8$  cells/mL suspension at 37  $^{\circ}\text{C}$  in a shaking water bath (75 rpm) for 24 h. The final cell concentration was  $7.2 \times 10^7$  erythrocytes/mL. The samples were collected over time, and percent hemolysis was determined as described above.

**Efficacy of PEO-*b*-p(HASA)/AmB.** Efficacy was assessed by organism killing in the kidneys of a neutropenic murine model of disseminated fungal infection as described previously by Andes et al.<sup>20–22</sup> A clinical isolate of *Candida albicans* (K-1) was grown and quantified on SDA. For 24 h prior to infection, the organism was subcultured at 35  $^{\circ}\text{C}$  on SDA slants. A  $10^6$  CFU/mL inoculum (CFU, colony forming units) was prepared by placing six fungal colonies into 5 mL of sterile, depyrogenated normal (0.9%) saline warmed to 35  $^{\circ}\text{C}$ . Six-week-old ICR/Swiss specific-pathogen-free female mice were obtained from Harlan Sprague Dawley (Madison, WI). All animal studies were approved by the Animal Research Committee of the William S. Middleton Memorial VA Hospital (Madison, WI). The mice were weighed (23–27 g) and given intraperitoneal injections of cyclophosphamide to render neutropenia. (For the purposes of this study, neutropenia was defined as  $<100$  polymorphonuclear leukocytes/ $\text{mm}^3$ .) Each mouse was dosed with 150 mg/kg of cyclophosphamide 4 days prior to infection and 100 mg/kg 1 day before infection. Disseminated candidiasis was induced via tail vein injection of 100  $\mu\text{L}$  of inoculum.

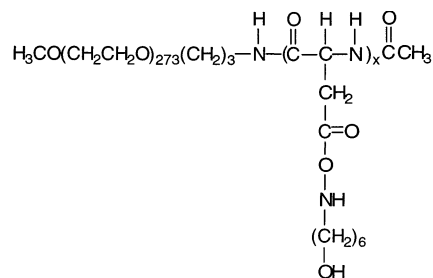
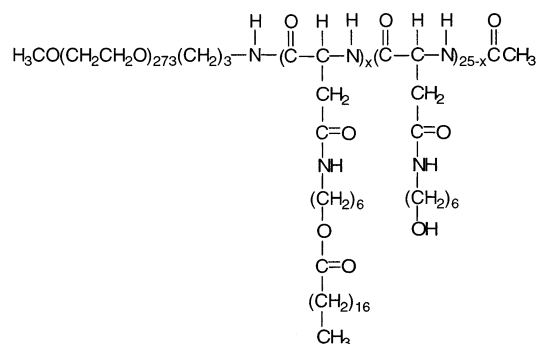
The AmB/polymeric micelle formulations or micelle blanks were reconstituted with 1.0 mL of 5% dextrose. The treatment group was given single 200  $\mu\text{L}$  intravenous (iv) injections of reconstituted AmB/PEO-*b*-p(HASA), 91% 2 h postinfection. Doses were calculated in terms of mg of AmB/kg of body weight. Control animals were given a placebo of "blank" polymeric micelles. Over time, two animals per experimental condition were sacrificed by CO<sub>2</sub> asphyxiation. The kidneys from each animal were removed and homogenized. The homogenate was diluted 10-fold with 9% saline and plated on SDA. The plates were then incubated for 24 h at 35  $^{\circ}\text{C}$  and inspected for CFU determination. The lower limit of detection for this technique is 100 CFU/mL. To compare the antifungal activity of the AmB/ micelle formula-



**Table 1.** Synthesis Products

polymer	stearic acid reacted, equiv of acid/equiv of OH	deg of substitution, av $\pm$ std dev <sup>b</sup>	x <sup>c</sup>
PEO- <i>b</i> -p(6-HHA)	n/a <sup>a</sup>	99.3 $\pm$ 0.5	25
PEO- <i>b</i> -p(HASA), 46%	0.5	46.3 $\pm$ 1.0	12
PEO- <i>b</i> -p(HASA), 91%	5	90.7 $\pm$ 0.9	23

<sup>a</sup> Not applicable. <sup>b</sup> Determined by <sup>1</sup>H NMR (Varian, 500 MHz) from five integrations per polymer batch. <sup>c</sup> Refers to Figure 1 and represents the average number of conjugated groups per 25 L-Asp repeat units.

A. PEO-*b*-p(6-HHA).B. PEO-*b*-p(HASA).**Figure 1.** Chemical structures of polymers used for encapsulation of AmB.

lations with that of Fungizone, animals were dosed with equivalent doses of AmB as Fungizone as described above. The control animals for the Fungizone group received 200  $\mu\text{L}$  iv injections of 5% dextrose. All results are expressed as the mean CFU per kidney for two animals (four kidneys total). The change in the area under the time–kill curves was calculated by  $\Delta\text{AUC}_{\text{TK}} = \text{AUC}_{\text{control}} - \text{AUC}_{\text{treatment}}$ . Outcomes were compared using ANOVA on ranks.

## Results and Discussion

**Polymer Preparation.** PEO-*b*-p(6-HHA) was prepared by aminolysis of PEO-*b*-PBLA with 6-aminohexanol. The product was then reacted with stearic acid in order to prepare PEO-*b*-p(HASA) at two different esterification levels. The average degree of substitution for each step was determined using <sup>1</sup>H NMR spectroscopy (Table 1). Parts A and B of Figure 1 contain the structures for PEO-*b*-p(6-HHA) and PEO-*b*-p(HASA), respectively. For the esterified polymers, the degree of stearate attachment was either 46 or 91%.

**Micelle Stability.** Polymeric micelles were prepared and stored in the solid state. Upon reconstitution with 1.0 mL of PBS, all formulations yielded clear solutions. The reconstituted solutions contained 0.5 and 10.0 mg/mL of PEO-*b*-

**Table 2.** SEC Results for Polymeric Micelle Samples with and without AmB

esterification level, %	AmB:polymer, mol:mol	10 <sup>6</sup> M <sub>w</sub> , g/mol	10 <sup>6</sup> M <sub>n</sub> , g/mol	polydispersity
0	0.0	n/a	n/a	n/a
0	0.1	n/a	n/a	n/a
46	0.0	3.9	1.6	2.4
46	1.9	2.5	1.5	1.7
91	0.0	5.0	2.4	2.1
91	1.2	4.9	2.1	2.3
91	2.0	4.7	2.0	2.3
91	3.6	2.9	1.8	1.6

**Table 3.** Encapsulation of AmB as a Function of Stearate Attachment

esterification level, %	[polymer], mg/mL <sup>a</sup>	[AmB], $\mu\text{M}$ <sup>a</sup>	AmB:polymer, mol:mol	encapsulation efficiency
0	10	44.9 $\pm$ 0.8	0.08 $\pm$ 0.01	0.66 $\pm$ 0.01
46	0.5	47.2 $\pm$ 1.8	1.91 $\pm$ 0.07	0.70 $\pm$ 0.03
91	0.5	42.7 $\pm$ 0.3	1.96 $\pm$ 0.01	0.63 $\pm$ 0.01

<sup>a</sup> Upon reconstitution with 1.0 mL of d.H<sub>2</sub>O.

p(HASA) and PEO-*b*-p(6-HHA), respectively. The critical micelle concentration (cmc) is the concentration at which micelle formation begins in aqueous solution and is related to the thermodynamic equilibrium between micelles and unimers, i.e., thermodynamic stability. A 20-fold excess of PEO-*b*-p(6-HHA) compared to PEO-*b*-p(HASA) was used for AmB encapsulation in order to account for the differences observed previously in the magnitudes of the cmc's and ensure micelle formation.<sup>17</sup> In addition, structure–property studies conducted with poly(ethylene oxide)-*block*-poly(*N*-hexyl-L-aspartamide)-acyl conjugate micelles indicated that PEO-*b*-p(6-HHA) micelles contain more fluid core regions than those assembled from the esterified diblock copolymers.<sup>17</sup> Therefore, PEO-*b*-p(6-HHA) micelles might be less kinetically stable than micelles formed by the esterified polymers. Due to decreased thermodynamic and kinetic stability, it is reasonable to expect that micelles prepared from PEO-*b*-p(6-HHA) might dissociate rapidly upon dilution. While it was possible to approximate the molecular weight for the PEO-*b*-p(HASA) micelles by GPC, PEO-*b*-p(6-HHA) micelles were indeed unstable and did not remain intact on the column (Table 2). Esterification of PEO-*b*-p(6-HHA) with stearic acid at 46 and 91% substitution imparted the stability necessary to withstand dilution on the column (Table 2). Generally, the molecular weight of polymeric micelles as determined by GPC analysis is on the order of 10<sup>6</sup> g/mol.<sup>19,23</sup>

### Encapsulation and Relative Aggregation State of AmB.

For all esterification levels studied (0, 46, and 91%), AmB was encapsulated with similar loading efficiency (Table 3). For the acylated polymers, the drug level is substantially higher than that achieved in previous efforts, which resulted in approximately 0.2–0.9 AmB:polymer on a mole to mole basis.<sup>16</sup> Improved assembly conditions are likely responsible for the increased drug-to-polymer ratios. Although the final AmB concentration in each formulation in the present study was similar, the AmB:polymer molar ratio is very low (approximately 0.1) for PEO-*b*-p(6-HHA). These results

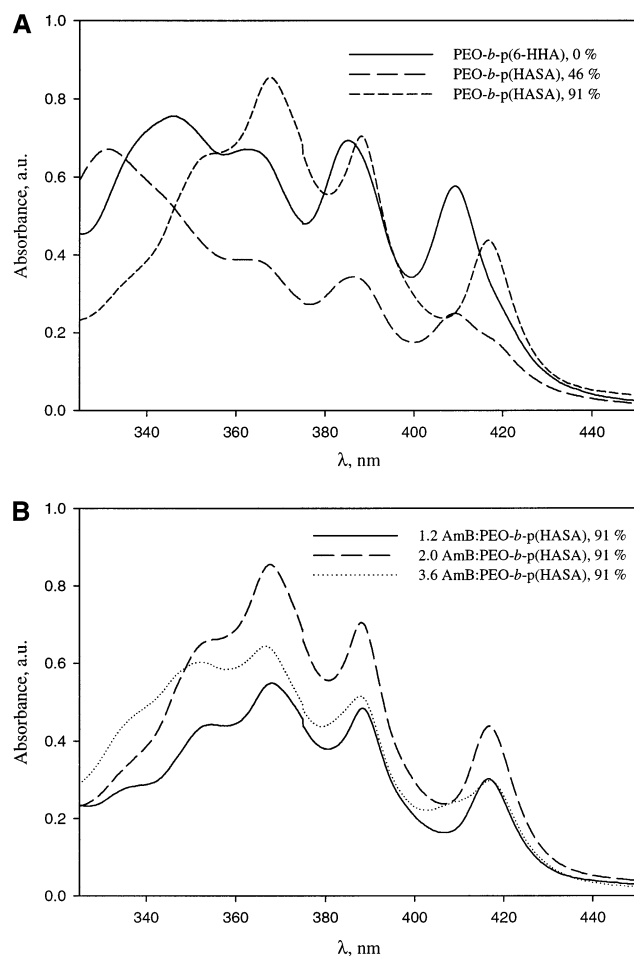


**Figure 2.** (A) Absorption spectrum of encapsulated AmB as a function of stearate esterification. (B) Absorption spectrum of AmB encapsulated by PEO-*b*-p(HASA), 91% as a function of drug level.

indicate that PEO-*b*-p(6-HHA) micelles have a low capacity for AmB solubilization.

The absorption spectrum of AmB is quite sensitive to changes in the local environment.<sup>24</sup> Hence, the relative self-aggregation state of the drug may be monitored via absorption spectroscopy. In fact, the relative intensity ratio of the first (346 nm) to the fourth band (409 nm), often referred to as the I/IV ratio, serves as a measure of AmB aggregation state. This ratio is  $<0.25$  for monomeric, or nonaggregated, AmB and may be as high as 2.0 for highly aggregated species.<sup>25</sup> Because all of the copolymers used in the present study have the same 12 000 g/mol PEO hydrophilic block, 25 repeat-unit poly(L-Asp) backbone, and hexyl spacer, the differences between the formulations may be attributed to relative level of stearate attachment. The absorption spectrum of AmB encapsulated by PEO-*b*-p(6-HHA) and PEO-*b*-p(HASA), 46 and 91%, is given in Figure 2A. The absorption spectrum of AmB encapsulated in the unesterified PEO-*b*-p(6-HHA) micelles is characterized by four bands at 346, 362, 385, and 409 nm. In addition, the I/IV ratio is 1.2 and indicative of a reduction in the self-aggregation state of the drug.

The effects of stearate conjugation on the relative aggregation state of AmB are quite apparent. For polymeric micelles containing 46% stearate attachment, the absorption spectrum of encapsulated AmB is characterized by strong

**Table 4.** Effect of Loading Conditions on AmB Encapsulation by PEO-*b*-p(HASA), 91%

initial level of AmB, $\mu\text{g}$	MeOH vol, mL	[AmB] loaded, $\mu\text{g/mL}^a$	AmB:PEO- <i>b</i> -p(HASA), 91%, mol:mol	encapsulation efficiency
625	4.0	$26.4 \pm 1.0$	$1.2 \pm 0.1$	$0.39 \pm 0.01$
625	2.0	$42.7 \pm 0.3$	$2.0 \pm 0.1$	$0.63 \pm 0.01$
1250	4.0	$78.5 \pm 2.8$	$3.6 \pm 0.1$	$0.58 \pm 0.01$

<sup>a</sup> Upon reconstitution with 1.0 mL of d.H<sub>2</sub>O.

absorption in the 330–340 nm region and indicative of highly self-aggregated species (Figure 2A). However, the fourth absorption band in the spectrum contains a shoulder at higher wavelengths. Hence, there may be a small quantity of less self-aggregated drug species. At 91% esterification, the absorption spectrum of encapsulated AmB is characterized by peaks at 354, 368, 388, and 417 nm (Figure 2A). This finding confirms previous studies, which indicated that increased esterification with stearate side chains results in a reduction in AmB self-aggregation.<sup>16</sup> Furthermore, the  $\lambda_{\text{max}}$  is red-shifted to 368 nm, and the absorption bands are narrower than those observed when AmB is encapsulated by PEO-*b*-p(6-HHA) and PEO-*b*-p(HASA), 46%. This spectrum bears striking similarity to that observed when AmB is complexed with ergosterol.<sup>24,26</sup> Therefore, we postulate that AmB may interact strongly with the stearate side chains of micelles prepared from highly substituted PEO-*b*-p(HASA).

The effects of initial loading conditions on the final AmB level in PEO-*b*-p(HASA), 91% micelles are given in Table 4. The corresponding absorption spectra are given in Figure 2B. For lower AmB/PEO-*b*-p(HASA), 91% ratios (1.2 and 2.0), the absorption spectrum is very similar to that obtained from AmB/ergosterol complexes as mentioned above. However, at a loading level of 3.6 AmB/polymer, an increase in absorption intensity is observed in the 330 nm region of the spectrum. In addition, the absorption bands are broader than those of the other PEO-*b*-p(HASA), 91% formulations. Taken together, these spectral features indicate a possible threshold level for the interaction of AmB with the stearate side chains of PEO-*b*-p(HASA) micelles. It is possible that AmB begins to self-associate at high levels of drug loading.

**Hemolytic Profile.** The hemolytic profiles of the polymeric micelle formulations indicate time-dependent activity and, likely, sustained drug release. For the formulations containing PEO-*b*-p(6-HHA) or PEO-*b*-p(HASA), 46% micelles in the absence of AmB, no hemolysis was observed over the course of 24 h (data not shown). However, slight hemolysis (approximately 4%) was observed in the presence of PEO-*b*-p(HASA), 91% after 16 h. Therefore, the leakage of hemoglobin from the bovine erythrocytes is attributed to action of AmB on the cell membranes. At similar drug levels (approximately 3  $\mu\text{g/mL}$ ), the onset of hemolysis is more gradual for the PEO-*b*-p(HASA), 91% formulation than for those with 0 and 46% stearate attachment (Figure 3). When taken in conjunction with the corresponding absorption spectra, this finding supports interaction between the stearate side chains of PEO-*b*-p(HASA) and AmB.

Free AmB caused 40% hemolysis after 1 h and nearly 80% hemolysis after 9 h (Figure 3). The onset of hemolytic activity was delayed upon encapsulation in all of the

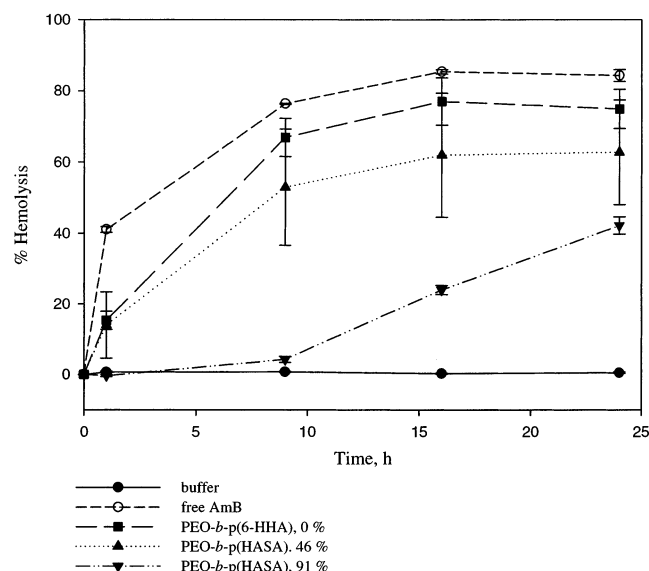


**Figure 3.** Hemolytic activity of 3 µg/mL AmB against  $7.2 \times 10^7$  bovine erythrocytes/mL over time as a function of stearate attachment.

polymeric micelles studied, regardless of the aggregation state of the drug. Although PEO-*b*-p(6-HHA) encapsulation seems to lead to relatively low levels of drug self-aggregation as evidenced by the corresponding absorption spectrum (Figure 2A), hemolytic activity is readily apparent. Such rapid hemolysis is likely due to instability of the PEO-*b*-p(6-HHA) micelles. As discussed previously, GPC studies indicated rapid dissociation of the PEO-*b*-p(6-HHA) micelle structures. Consequently, AmB-induced hemolysis occurs quickly.

The hemolytic profile of the AmB/PEO-*b*-p(HASA), 46% formulation is similar to that observed with the unesterified polymer formulation. While 46% stearate esterification increased micelle stability as evidenced by GPC analysis, it had little impact on the time-dependent hemolytic activity of AmB. Absorption spectroscopy indicated that AmB was encapsulated by PEO-*b*-p(HASA), 46% in a self-aggregated state (Figure 2A). Therefore, it is likely that the drug was released as an aggregated species, which would be capable of inducing rapid hemolysis of mammalian cells. On the other hand, AmB encapsulated at the same level by 91% esterified polymer had a markedly different hemolytic profile with 4% hemolysis at 9 h, 20% at 16 h, and 40% at 24 h (Figure 3). In this case, the absorption spectrum of encapsulated AmB (Figure 2A) indicated that the drug was encapsulated in a non-self-aggregated state. Hence, it is reasonable to propose that the gradual build-up of hemolytic activity observed when AmB was encapsulated in highly substituted polymeric micelles is due to the sustained release of relatively non-aggregated species.

The onset of hemolysis for AmB encapsulated by PEO-*b*-p(HASA), 91%, was delayed compared to equivalent concentrations of free AmB (Figure 4). At all concentrations studied, the onset of hemolysis is delayed when AmB is encapsulated in PEO-*b*-p(HASA), 91%. On the other hand, the level of drug loading in PEO-*b*-p(HASA), 91% micelles, did impact the time-dependent hemolytic profile. At lower drug levels (1.2 and 2.0 drug/polymer), the profiles are nearly

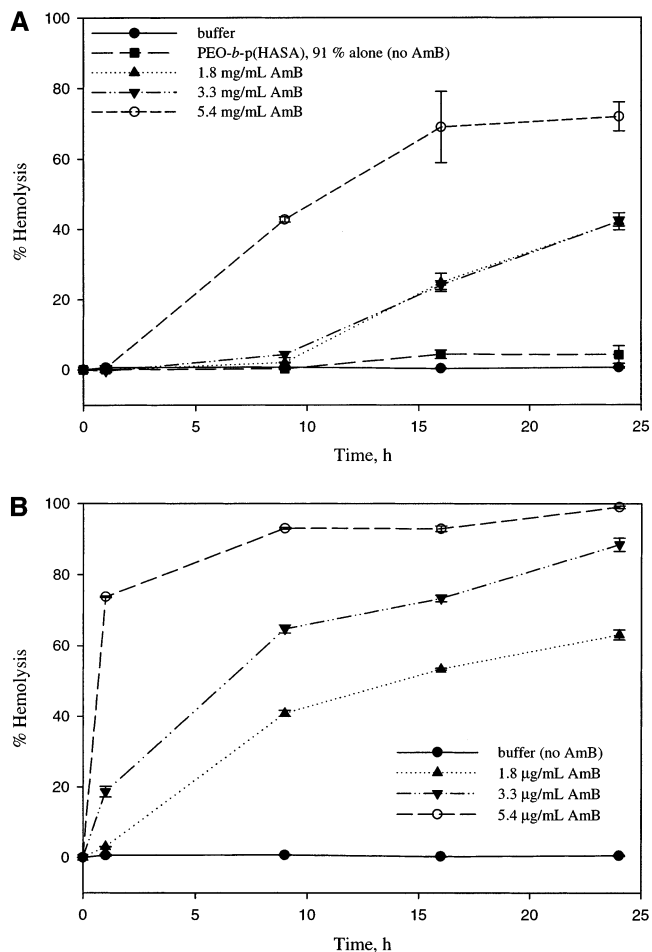


**Figure 4.** (A) Hemolytic activity of AmB encapsulated by PEO-*b*-p(HASA), 91% micelles as a function of time and drug level. (B) Hemolytic profile of free AmB over time against bovine erythrocytes.

identical with very little hemolysis at 9 h, 20% at 16 h, and approximately 40% at 24 h (Figure 4A).

However, the onset of hemolysis is more rapid at an AmB/polymer loading level of 3.6. These findings correlate with the corresponding absorption spectra (Figure 2B), which suggest that AmB self-aggregation begins to occur at high drug levels, i.e., 3.6 AmB/PEO-*b*-p(HASA), 91%. It is plausible that AmB is released slowly from PEO-*b*-p(HASA), 91% micelles. However, at high drug levels, AmB may be released as a more aggregated species or in quantities that more quickly surpass the threshold required for self-aggregation in aqueous media. As a result, toxicity toward mammalian cells, as evidenced by hemolysis of bovine erythrocytes, becomes apparent.

**Efficacy.** Fungal growth curves for both treated and control animals following single iv doses of AmB are given in Figure 5.

Following tail vein inoculation, growth of *C. albicans* in the kidneys of both groups increased (3.2–3.5 log CFU/kidney) over the time period of the studies. The infection level (CFU<sub>kidney</sub>) is similar to that obtained in previous studies using the same murine model, which resulted in approximately 3.5–4.5 CFU<sub>kidney</sub> 2 h following inoculation.<sup>20–22</sup> Treatment with both AmB/PEO-*b*-p(HASA), 91%, and AmB as Fungizone suppressed organism growth in a dose-dependent manner at the doses studied. Kidney CFU deter-

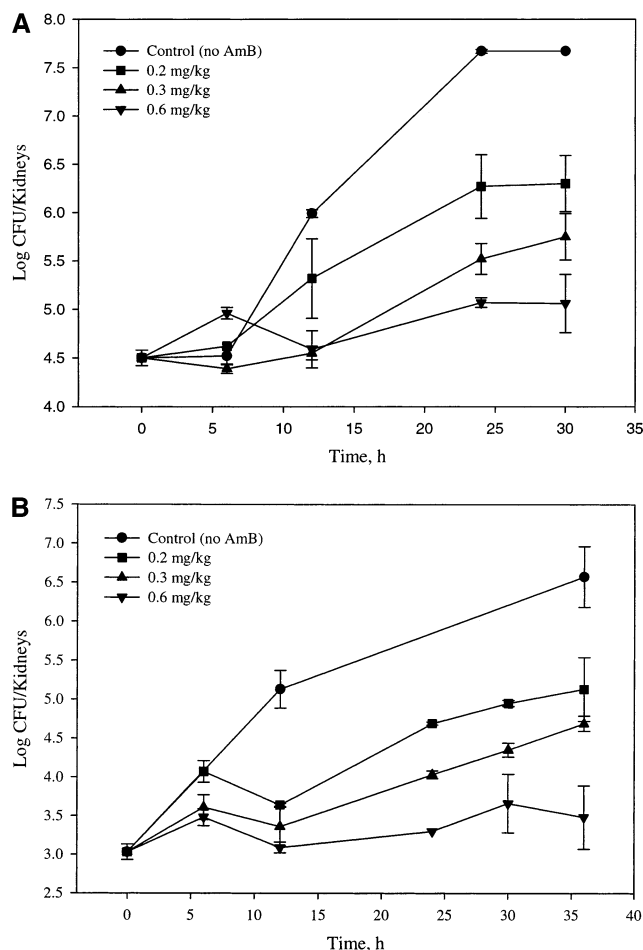


**Figure 5.** In vivo time-kill plots for AmB as a function of dose in a neutropenic murine model of disseminated candidiasis: (A) AmB encapsulated by PEO-*b*-p(HASA), 91% micelles; (B) AmB as Fungizone.

mination indicated that the efficacy of AmB encapsulated by PEO-*b*-p(HASA), 91%, was not significantly different than that of Fungizone at doses of 0.2, 0.3, and 0.6 mg/kg of AmB ( $p = 0.70$ ). Hence, encapsulation of AmB by PEO-*b*-p(HASA), 91% micelles, did not have a detrimental effect on the potent antifungal activity of AmB in a neutropenic murine model of disseminated fungal infection. These results contrast to those obtained for conventional liposomal AmB (AmBisome), of which higher doses are required to obtain equivalent efficacy to Fungizone.<sup>4</sup> On the other hand, PEGylated liposomes are more efficacious than AmBisome, presumably due to prolonged circulation time.<sup>11</sup> Due to high thermodynamic and kinetic stability in combination with a high surface density of PEO chains, AmB encapsulated by PEO-*b*-p(HASA), 91% micelles, may be long circulating and released gradually over time. As this scenario may account for the retained potency of AmB encapsulated by PEO-*b*-p(HASA) micelles, the residence time of the polymeric micelle formulation will be explored in future work.

### Conclusions

It is possible to formulate AmB via a polymeric micelle system based on PEO-*b*-p(L-Asp) derivatives. Under the experimental conditions, PEO-*b*-p(HASA) assembles into

kinetically stable supramolecular structures capable of encapsulating AmB. Encapsulation of AmB by PEO-*b*-p(HASA) micelles alters the self-association behavior of AmB compared to free drug, likely due to interactions or complexation between the stearate side chains and AmB. Through manipulation of initial loading conditions and altering the extent of stearate esterification, it is possible to exercise some measure of control over the aggregation state of AmB. As the self-aggregation state of the drug has proven to be a good indicator of toxicity and hemolytic activity, encapsulation of AmB in PEO-*b*-p(HASA) micelles with high levels of stearate attachment might be capable of reducing the toxicity of AmB toward mammalian cells. The ability to alter the equilibrium between the various aggregates might prove quite powerful in terms of drug delivery.

Interactions between highly substituted PEO-*b*-p(HASA), as indicated by absorption spectroscopy, may result in sustained release of relatively non-self-aggregated AmB, hence the delayed onset of hemolysis. AmB was released from the micelles in vivo (bioavailable) by or around 6 h based upon time of organism suppression. In vivo time-kill studies suggest that the AmB/PEO-*b*-p(HASA), 91% formulation, is as efficacious as Fungizone, the standard clinical formulation of AmB, against *C. albicans* in a neutropenic murine model of systemic fungal infection. Our polymeric micelle formulation has the advantage of reconstitutability after storage in the solid state. Consequently, long-term solution phase stability is not necessary. PEO-*b*-p(HASA), 91% micelles, might possess the stability to withstand in vivo dilution and be capable of sustained release of AmB. Ultimately, via tailoring the formulation through control over micelle stability, AmB self-aggregation state, and final drug level, it might be possible to improve the selectivity of AmB for fungal cell membranes. The in vivo toxicity of AmB/PEO-*b*-p(HASA), 91% micelles, and plasma concentration-time profile will be assessed in future work.

**Acknowledgment.** This work was funded by NIH Grant AI-43346-02. The authors wish to thank NanoCarrier, Inc. (Japan), for kindly supplying PEO-*b*-PBLA.

### References and Notes

- (1) Saral, R. *Rev. Infect. Dis.* **1991**, *13*, 487.
- (2) Groll, A. H.; Piscitelli, S. C.; Walsh, T. J. In *Clinical Pharmacology of Systemic Antifungal Agents: A Comprehensive Review of Agents in Clinical Use, Current Investigational Compounds, and Putative Targets for Antifungal Drug Development*; August, J. T., Anders, M. W., Murad, F., Coyle, J. T., Eds.; Advances in Pharmacology 44; Academic Press: San Diego, CA, 1998; pp 343–500.
- (3) Hartsel, S.; Bolard, J. *Trends Pharmacol. Sci.* **1996**, *17*, 445.
- (4) White, M. H. In *Progress in the use and delivery of polyenes in antifungal therapy*; Dixon, G. K., Copping, L. G., Hollomon, D. W., Eds.; Antifungal Agents: discovery and mode of action; BIOS Scientific Publishers Limited: Oxford, 1995; pp 69–75.
- (5) Dupont, B. *J. Antimicrob. Chemother.* **2002**, *49* Suppl. S1, 31.
- (6) Cleary, J. D.; Chapman, S. W.; Clark, A.; Lucia, H. Fungal Infections. In *Applied Therapeutics, The Clinical Use of Drugs*, 7th ed.; Mary Anne Koda-Kimble, Lloyd Yee Young, Eds.; Wayne A. Kradjan, B. Joseph Guglielmo, Assoc. Eds.; Lippincott Williams and Wilkins: Philadelphia, PA, 2001; Chapter 16.
- (7) van Etten, E. W. M.; van Vianen, W.; Tjhuis, R. H. G.; Storm, G.; Bakker-Woudenberg, I. A. J. *M. J. Controlled Release* **1995**, *37*, 123.
- (8) van Etten, E. W. M.; Snijders, S. V.; van Vianen, W.; Bakker-Woudenberg, I. A. J. *M. J. Antimicrob. Agents Chemother.* **1995**, *42* (9), 1954.



- (9) Bakker-Woudenberg, I. A. J. M. *Int. J. Antimicrob. Agents* **2002**, *19*, 299.
- (10) van Etten, E. W. M.; Stearne-Cullen, E. T.; ten Kate, M. T.; Bakker-Woudenberg, I. A. J. M. *Antimicrob. Agents Chemother.* **2000**, *44* (3), 540.
- (11) van Etten, E. W. M.; ten Kate, M. T.; Stearne, L. E. T.; Bakker-Woudenberg, I. A. J. M. *Antimicrob. Agents Chemother.* **1995**, *39* (9), 1954.
- (12) Kataoka, K.; Harada, A.; Nagasaki, Y. *Adv. Drug Delivery Rev.* **2001**, *47*, 113.
- (13) Allen, C.; Maysinger, D.; Eisenberg, A. *Colloids Surf., B* **1999**, *16*, 3.
- (14) Jeon, S. I.; Lee, J. H.; Andrade, J. D.; De Gennes, P. G. *J. Colloid Interface Sci.* **1991**, *142* (1), 149–158.
- (15) Kwon, G. S.; Suwa, S.; Yokoyama, M.; Okano, T.; Sakurai, Y.; Kataoka, K. *J. Controlled Release* **1994**, *29*, 17.
- (16) Lavasanifar, A.; Samuel, J.; Sattari, S.; Kwon, G. S. *Pharm. Res.* **2002**, *19* (4), 418.
- (17) Adams, M. L.; Kwon, G. S. *J. Biomater. Sci., Polym. Ed.* **2002**, *13* (9), 991.
- (18) Lavasanifar, A.; Samuel, J.; Kwon, G. S. *J. Controlled Release* **2001**, *77*, 155.
- (19) Adams, M. L.; Kwon, G. S. *J. Controlled Release* **2003**, *87*, 23.
- (20) Andes, D.; Stamsted, T.; Conklin, R. *Antimicrob. Agents Chemother.* **2001**, *45* (3), 922.
- (21) Andes, D.; van Ogtrop, M. *Antimicrob. Agents Chemother.* **2000**, *44* (4), 938.
- (22) Andes, D.; van Ogtrop, M. *Antimicrob. Agents Chemother.* **1999**, *43* (9), 2116.
- (23) Yamamoto, Y.; Yasugi, K.; Harada, A.; Nagasaki, Y.; Kataoka, K. *J. Controlled Release* **2002**, *82*, 359.
- (24) Gruda, I.; Dussault, N. *Biochem. Cell Biol.* **1988**, *66*, 177.
- (25) Barwicz, J.; Christian, S.; Gruda, I. *Antimicrob. Agents Chemother.* **1992**, *36* (10), 2310.
- (26) Charbonneau, C.; Fournier, I.; Dufresne, S.; Barwicz, J.; Tancrede, P. *Biophys. Chem.* **2001**, *91*, 125.

BM0257614